THE ASTROPHYSICAL JOURNAL, 416:752–761, 1993 October 20

FINITE-VELOCITY EFFECTS ON ATOMS IN STRONG MAGNETIC FIELDS AND IMPLICATIONS FOR NEUTRON STAR ATMOSPHERES

G. G. PAVLOV[1,2] AND P. MÉSZÁROS[1]
Received 1993 January 20; accepted 1993 April 27

ABSTRACT

We consider the effects of a finite velocity on the properties of atoms in the strong magnetic field characteristic of neutron stars. Whereas in the absence of significant center-of-mass velocities the atomic structure is determined by the cylindrical symmetry, the electric field induced by the finite motion breaks this symmetry and distorts the atomic structure. The resulting dependence of the total energy on a generalized momentum of the atom can be interpreted in terms of a mass anisotropy—the atom becomes "heavier" when it moves across the magnetic field, the transverse mass being higher for the more excited states. The field-dependent mass anisotropy, together with the field dependence of the binding energy of the atom, leads to a bending of the trajectories of neutral atoms in nonuniform magnetic fields, tending to channel and retain them in regions of high field. It also leads to a number of thermodynamic and spectroscopic effects. In particular, the mass anisotropy introduces both quantitative spectroscopic changes relative to the stationary magnetized atom, such as additional shifts and broadening of photoionization edges and lines, as well as qualitative changes, such as new selection rules for radiative processes and for the annihilation of magnetic positronium. The ionization balance of atoms and ions in pulsar atmospheres may also be strongly influenced, which together with the opacity changes could lead to effects of significant importance for the modeling of neutron star atmospheres in magnetic fields of strength $B \gtrsim 10^9$ G.

Subject headings: atomic processes — magnetic fields — pulsars: general — stars: neutron

1. INTRODUCTION

The structure of atoms at rest in a magnetic field $\beta \equiv \hbar\omega_{Be}/4$ Ry $= B/4.7 \times 10^9$ G is of great astrophysical interest. In the usual (stellar atmosphere or laboratory) case $\beta \ll 1$ one obtains the well-known Zeeman effect as a perturbation of the nonmagnetic atomic structure, which does not significantly distort the geometry of the atom. In the strong (e.g., pulsar) case $\beta \gtrsim 1$, the structure of the atomic levels is entirely different from the Zeeman scheme, and the atom acquires a definite cylindrical structure (e.g., Ruderman 1974; Canuto & Ventura 1977; Herold, Ruder, & Wunner 1981; Mészáros 1992 and references therein). However, most of the previous work on the strong field case neglects the fact that if the motion of the atoms is taken into account, a transverse electric field $\boldsymbol{E} = (\boldsymbol{v}/c) \times \boldsymbol{B}$ appears in the rest frame of the atom, which if sufficiently strong will distort the eigenfunction and energy spectrum, and will break the axial symmetry of the problem.

A first important step in this problem was taken by Gor'kov & Dzyaloshinskii (1968), who found an integral of the motion $\boldsymbol{P}$ of the neutral two-body system in a magnetic field that plays the role of the momentum of the system. They also suggested an approach to separate the center-of-mass motion and obtained a Schrödinger equation for the relative motion. Some general mathematical aspects of this problem were further explored by Avron, Herbst, & Simon (1978). Herold et al. (1981) considered the two-body problem in the special case of a harmonic interaction between the particles and analyzed the effect of the finite proton mass on the energy spectrum of a hydrogen atom moving parallel to the magnetic field ($\boldsymbol{P}_\perp = 0$). Vincke & Baye (1988) obtained the first quantitative results on the spectrum of the hydrogen atom moving across the magnetic field. They applied the perturbation approach, which leads to a quadratic dependence of the energy correction on $\boldsymbol{P}_\perp$, and calculated the field dependence of the effective "transverse" mass of the atom for the four lowest tightly bound levels. As a zero approximation, they used wave functions and energies of the fixed atom calculated with a variational method.

Although the perturbation approach is valid only for transverse atomic velocities that are not too high, it allows one to understand many qualitative effects of the atomic motion that are important for astrophysical applications. The anisotropy of the atomic mass in a magnetic field should obviously lead to qualitative differences in the kinematics of the atomic motion, change the thermodynamic properties of plasmas in neutron star atmospheres (e.g., ionization equilibrium), and give rise to new spectroscopic effects potentially important for the interpretation of soft X-ray/UV/optical observations of neutron stars. These effects and their astrophysical implications have not been discussed so far.

In the present paper we extend the investigation of the physics of the atomic motion in magnetic fields, both qualitatively and quantitatively (§ 2). In particular, we investigate the dependence of the transverse atomic mass on the magnetic field, not only for the tightly bound levels but also for the hydrogen-like levels, making use of numerical solutions of the Schrödinger equation for a fixed atom. We consider also the motion of positronium in a magnetic field, which represents a special case due to equality of the e^+ and e^- masses. We then discuss different macroscopic consequences of the anisotropy of the atomic mass (§ 3), both in general and for pulsar environments. The applications of these results to specific astrophysical problems are discussed in § 4, including possible observational consequences.

[1] Pennsylvania State University, 525 Davey Laboratory, University Park, PA 16802
[2] Ioffe Physico-Technical Inst., Russian Academy of Sciences, 194021 St. Petersburg, Russia

2. QUANTUM MECHANICS OF MOVING MAGNETIZED ATOMS

2.1. *Generalized Momentum of a System of Charged Particles*

To treat the N-body problem in a magnetic field, it is necessary first to search for appropriate conserved quantities. The velocity of the center of mass is not an integral of the motion, in this case. This can be seen by considering the kinetic momentum operator in a magnetic field for each particle i

$$\hat{\boldsymbol{\pi}}_i = \hat{\boldsymbol{p}}_i - (e_i/c)\boldsymbol{A}(\boldsymbol{r}_i) , \tag{2.1}$$

which defines a total kinetic momentum for the atom

$$\hat{\boldsymbol{P}}_{\rm kin} = \sum_{i=1}^{N} \hat{\boldsymbol{\pi}}_i = M\dot{\boldsymbol{R}} . \tag{2.2}$$

where $\hat{\boldsymbol{p}}_i = -i\hbar(\partial/\partial \boldsymbol{r}_i)$ is the canonical momentum, $M = \sum_i m_i$ is the total mass of the system, $\boldsymbol{R} = M^{-1}\sum_i m_i \boldsymbol{r}_i$ is the center-of-mass position. Using the Hamiltonian operator

$$\hat{H} = \sum_{i=1}^{N} \frac{\hat{\boldsymbol{\pi}}_i^2}{2m_i} + V(\boldsymbol{r}_1, \ldots \boldsymbol{r}_N) , \tag{2.3}$$

one sees that the commutator of the total kinetic momentum operator and of the Hamiltonian does not vanish,

$$\dot{\hat{\boldsymbol{P}}}_{\rm kin} = \frac{1}{i\hbar}[\hat{\boldsymbol{P}}_{\rm kin}, \hat{H}] = \sum_i \frac{e_i}{m_i} \hat{\boldsymbol{\pi}}_i \times \boldsymbol{B} , \tag{2.4}$$

and therefore $\boldsymbol{P}_{\rm kin}$ (or $\dot{\boldsymbol{R}}$) is not a conserved quantity.

However, it is possible to define a total generalized momentum $\boldsymbol{P}$ through

$$\hat{\boldsymbol{P}} = \hat{\boldsymbol{P}}_{\rm kin} + \sum_{i=1}^{N} \frac{e_i}{c} \boldsymbol{B} \times \boldsymbol{r}_i = \sum_i \left(\hat{\boldsymbol{p}}_i - \frac{e_i}{c}\boldsymbol{A}_i + \frac{e_i}{c}\boldsymbol{B} \times \boldsymbol{r}_i \right)$$

$$= \sum_i \left(\hat{\boldsymbol{p}}_i + \frac{e_i}{2c} \boldsymbol{B} \times \boldsymbol{r}_i \right) , \tag{2.5}$$

where $\boldsymbol{A}_i = \boldsymbol{A}(\boldsymbol{r}_i)$, and the latter equality implies the cylindrical gauge $\boldsymbol{A}_i = (\frac{1}{2})\boldsymbol{B} \times \boldsymbol{r}_i$. This satisfies

$$[\hat{\boldsymbol{P}}, \hat{H}] = 0 , \tag{2.6}$$

so $\boldsymbol{P}$ is an integral of the motion (Gor'kov & Dzyaloshinskii 1968; Avron et al. 1978; Herold et al. 1981). In addition, the individual components of the pseudomomentum also commute with each other,

$$[\hat{P}_\mu, \hat{P}_\nu] = -\frac{i\hbar}{c} \epsilon_{\mu\nu\lambda} B_\lambda \left(\sum_i e_i \right) \to 0 , \tag{2.7}$$

provided that the atom is electrically neutral.

2.2. *Perturbation Treatment of the Neutral Two-Body System*

The neutral two-body system moving in a strong magnetic field provides the simplest example to illustrate the effects of nonnegligible velocities. Writing

$$\boldsymbol{r} = \boldsymbol{r}_e - \boldsymbol{r}_i , \quad \boldsymbol{R} = M^{-1}(m_e \boldsymbol{r}_e + m_i \boldsymbol{r}_i) , \tag{2.8}$$

for the relative position vector and the center-of-mass position of the system (subscript e stands for negative charge), we have for the total pseudomomentum

$$\hat{\boldsymbol{P}} = -i\hbar \frac{\partial}{\partial \boldsymbol{R}} - \frac{e}{2c} \boldsymbol{B} \times \boldsymbol{r} . \tag{2.9}$$

The eigenfunction of the Hamiltonian, $\hat{H}\Psi = E\Psi$, and of the generalized momentum, $\hat{\boldsymbol{P}}\Psi = \boldsymbol{P}\Psi$, can be written in a form separating the center-of-mass motion (Gor'kov & Dzyaloshinskii 1968)

$$\Psi(\boldsymbol{R}, \boldsymbol{r}) = \exp\left[\frac{i}{\hbar} \left(\hat{\boldsymbol{P}} + \frac{1}{2c} e\boldsymbol{B} \times \boldsymbol{r} \right) \cdot \boldsymbol{R} \right] \psi_{\boldsymbol{P}}(\boldsymbol{r}) , \tag{2.10}$$

where $\psi_{\boldsymbol{P}}(\boldsymbol{r})$ satisfies the Schrödinger equation

$$\hat{H}_{\boldsymbol{P}} \psi_{\boldsymbol{P}} = E\psi_{\boldsymbol{P}} , \quad \hat{H}_{\boldsymbol{P}} = \hat{H}_{\rm rel} + \hat{H}_{\rm coupl} + \frac{P^2}{2M} . \tag{2.11}$$

The first and second terms of the Hamiltonian $\hat{H}_{\boldsymbol{P}}$ describe the relative motion at $\boldsymbol{P} = 0$ and the coupling between this and center-of-mass motion,

$$\hat{H}_{\rm rel} = \frac{\hat{p}^2}{2\mu} + \frac{e}{2c}\left(\frac{1}{m_e} - \frac{1}{m_i} \right) \boldsymbol{B} \cdot (\boldsymbol{r} \times \hat{\boldsymbol{p}}) + \frac{e^2}{8\mu c^2} (\boldsymbol{B} \times \boldsymbol{r})^2 - \frac{e^2}{r} ; \tag{2.12a}$$

$$\hat{H}_{\rm coupl} = \frac{e}{Mc} (\boldsymbol{P} \times \boldsymbol{B}) \cdot \boldsymbol{r} . \tag{2.12b}$$

The dependence of E on $\boldsymbol{P}$ allows one to determine the mean velocity of the atom for a given $\boldsymbol{P}$

$$\langle \boldsymbol{V} \rangle = \frac{\partial E}{\partial \boldsymbol{P}} . \tag{2.13}$$

We treat now the coupling Hamiltonian as a perturbation; that is, we consider the energy eigenvalue and the eigenfunction to be given by a perturbation series

$$E = \frac{P^2}{2M} + \epsilon^{(0)} + \epsilon^{(1)} + \cdots ; \quad \psi = \psi^{(0)} + \psi^{(1)} + \cdots . \tag{2.14}$$

The zeroth order terms $\psi^{(0)}$, $\epsilon^{(0)}$ are the solutions of the Schrödinger equation when the coupling is neglected,

$$\hat{H}_{\rm rel} \psi_\kappa^{(0)} = \epsilon_\kappa^{(0)} \psi_\kappa^{(0)} , \tag{2.15}$$

where κ is a set of quantum numbers of the unperturbed (fixed) atom. The first-order energy correction drops out, $\epsilon_\kappa^{(1)} = \langle \kappa | \hat{H}_{\rm coupl} | \kappa \rangle = 0$, due to the vanishing of the matrix element of $\hat{H}_{\rm coupl}$ between states with equal projections of the angular momentum onto $\boldsymbol{B}$. The first nonzero coupling contributions are given by the second-order terms,

$$\epsilon_\kappa^{(2)} = \sum_{\kappa' \neq \kappa} \frac{|\langle \kappa | H_{\rm coupl} | \kappa' \rangle|^2}{\epsilon_\kappa^{(0)} - \epsilon_{\kappa'}^{(0)}} . \tag{2.16}$$

In a strong magnetic field ($\beta \gg 1$), when the adiabatic approximation is valid, an appropriate set of quantum numbers is

$$\kappa = \{N, s, \nu\} , \tag{2.17}$$

where $N = 0, 1, 2, \ldots$ is the number of the Landau level, $s = -m = -N, -N+1, \ldots$ is the negative of the angular momentum projection onto $\boldsymbol{B}$, and ν is the "longitudinal" quantum number which enumerates the eigenvalues $\epsilon_{Ns\nu}^{\parallel}$ of the (one-dimensional) Hamiltonian averaged over the transverse relative motion, $\hat{H}_{Ns}^{\parallel} = \hat{p}_z^2/2\mu + \langle Ns | (-e^2/r) | Ns \rangle$. For the discrete spectrum ($\epsilon_{Ns\nu}^{\parallel} < 0$), $\nu = 0, 1, 2, \ldots$ represents the number of nodes of the longitudinal eigenfunction with parity $(-1)^\nu$. At $\beta \to \infty$ the energies of the tightly bound states ($\nu = 0$) grow logarithmically, $-\epsilon_{Ns0}^{\parallel} \sim (\ln \beta)^2$ Ry, whereas the energies of the hydrogen-like states ($\nu \geq 1$) cluster around the values of the field-free hydrogen atomic levels. In terms of the magnetic

atomic states, the zeroth-order energy eigenvalue is given by (Herold et al. 1981)

$$\epsilon^{(0)}_{N,s,\nu} = \hbar\omega_{Be}(N + \tfrac{1}{2}) + \hbar\omega_{Bi}(N + s + \tfrac{1}{2}) + \epsilon^{\parallel}_{N,s,\nu} , \quad (2.18)$$

where $\omega_{Bi} = eB/m_i c = (m_e/m_i)\omega_{Be}$ is the ion cyclotron frequency. In the ground Landau level $N = 0$ we then have simply $s = 0, 1, 2, \cdots$, and the second-order terms of the perturbation expansion are given by

$$\epsilon^{(2)}_{s,\nu} = \sum_{N,s'\nu'} \frac{|\langle 0s\nu | H_{\rm coupl} | N's'\nu'\rangle|^2}{\epsilon^{\parallel}_{0s\nu} - \epsilon^{\parallel}_{N's'\nu'} - N'\hbar\omega_{Be} + (s - s' - N')\hbar\omega_{Bi}} , \quad (2.19a)$$

where the matrix elements are calculated with the zero-order wave functions

$$\langle \boldsymbol{r} | Ns\nu\rangle = \psi^{(0)}_{Ns\nu}(\rho, \phi, z) = \frac{e^{-is\phi}}{\sqrt{2\pi}} \frac{1}{a_M\sqrt{N!(N+s)!}} \xi^{-s/2} e^{\xi/2} \times \frac{d^N}{d\xi^N}(\xi^{N+s} e^{-\xi}) g_{Ns\nu}(z) , \quad (2.19b)$$

in which $\xi = \rho^2/2a_M^2$, $a_M = (c\hbar/eB)^{1/2}$ is a characteristic magnetic length, and $g_{Ns\nu}(z)$ is an eigenfunction of the one-dimensional Hamiltonian $\hat{H}^{\parallel}_{Ns}$. With the aid of the well-known expressions for the matrix elements of cyclic projections of the radius vector (see, e.g., Potekhin & Pavlov 1993) the second-order energy correction (eq. [2.19a]) can be computed to be

$$\epsilon^{(2)}_{s\nu} = -\frac{P_\perp^2}{2M}\hbar\omega_{B0} \times \sum_{\nu'}\left[\frac{(s+1)I^2_{0s\nu;0,s+1,\nu'}}{\chi_{0s\nu} - \chi_{0,s+1,\nu'} + \hbar\omega_{Bi}} - \frac{sI^2_{0s\nu;0,s-1,\nu'}}{\chi_{0,s-1,\nu'} - \chi_{0s\nu} + \hbar\omega_{Bi}} + \frac{I^2_{0s\nu;1,s-1,\nu'}}{\chi_{0s\nu} - \chi_{1,s-1,\nu'} + \hbar\omega_{Be}}\right] , \quad (2.20)$$

where we have used the definitions

$$\chi_{Ns\nu} = -\epsilon^{\parallel}_{Ns\nu} , \quad \omega_{B0} = eB/Mc = (m_e/M)\omega_{Be} , \quad (2.21)$$

and the overlapping integrals I are given by

$$I_{0s\nu,N's'\nu'} = \int_{-\infty}^{\infty} dz\, g^*_{0s\nu}(z) g_{N's'\nu'}(z) . \quad (2.22)$$

Note that these differ from zero only if ν and ν' have the same parity. The total energy corresponding to an eigenstate $\{N = 0, s, \nu\}$ is

$$E_{0s\nu}(\boldsymbol{P}) = \epsilon^{(0)}_{0s\nu} + \frac{P_z^2}{2M} + \frac{P_\perp^2}{2M^\perp_{s\nu}} ; \quad (2.23)$$

where in the last term we have defined the perpendicular component of the mass of the atom, $M^\perp_{s\nu}$ as

$$\left(\frac{M^\perp_{s\nu}}{M}\right)^{-1} \equiv \mu^{-1}_{s\nu} = 1 - \hbar\omega_{B0} \times \sum_{\nu'}\left[\frac{(s+1)I^2_{0s\nu;0,s+1,\nu'}}{\chi_{0s\nu} - \chi_{0,s+1,\nu'} + \hbar\omega_{Bi}} - \frac{sI^2_{0s\nu;0,s\pm1,\nu'}}{\chi_{0,s-1,\nu'} - \chi_{0s\nu} + \hbar\omega_{Bi}} + \frac{I^2_{0s\nu;1,s-1,\nu'}}{\chi_{0s\nu} - \chi_{1,s-1,\nu'} + \hbar\omega_{Be}}\right] . \quad (2.24)$$

It follows from the completeness property of the eigenfunctions $g_{Ns\nu}(z)$,

$$\sum_\nu g^*_{Ns\nu}(z) g_{Ns\nu}(z') = \delta(z - z') , \quad (2.25)$$

that

$$\sum_{\nu'} I^2_{0s\nu,N's'\nu'} = 1 . \quad (2.26)$$

With the aid of this relation, equation (2.24) can be transformed as follows:

$$\mu^{-1}_{s\nu} = \sum_{\nu'}\left\{\frac{m_i}{M}\left[\frac{(s+1)I^2_{0s\nu;0,s+1,\nu'}}{a^i_{0s\nu;0,s+1,\nu'} + 1} - \frac{sI^2_{0s\nu;0,s-1,\nu'}}{a^i_{0,s-1,\nu';0s\nu} + 1}\right] + \frac{m_e}{M}\frac{I^2_{0s\nu;1,s-1,\nu'}}{a^e_{0s\nu;1,s-1,\nu'} + 1}\right\} , \quad (2.27)$$

where $a^{e,i}_{0s\nu,N's'\nu'} = \hbar\omega_{Be,Bi}/(\chi_{0s\nu} - \chi_{N's'\nu'})$. If one formally lets $B \to \infty$, the coupling integrals simplify, $I_{0s\nu;N',s\pm1,\nu'} \to \delta_{\nu\nu'}$, and $a^{i,e}_{0s\nu;N',s\pm1,\nu} \gg 1$, so that in this limit the mass anisotropy ratio $\mu_{s\nu} \to \infty$. In the opposite limit of comparatively low magnetic fields, $a_{0s\nu,N's'\nu'} \ll 1$, the anisotropy is very small, $\mu_{s\nu} \simeq 1$.

To calculate the longitudinal energies and overlapping integrals for arbitrary m_i and m_e, one can use these quantities calculated in the well-investigated limit $m_i \to \infty$, together with the scaling laws (cf. Wunner, Ruder, & Herold 1981a),

$$\chi_{Ns\nu}(B) = \lambda\chi_{Ns\nu}(B/\lambda^2, m_i \to \infty) , \quad (2.28a)$$

$$I_{Ns\nu,N's'\nu'}(B) = I_{Ns\nu,N's'\nu'}(B/\lambda^2, m_i \to \infty) , \quad (2.28b)$$

where $\lambda = m_i/M$.

The perturbation approach is justified as long as $|\epsilon^{(2)}_{0s\nu}| \ll |\Delta\epsilon^{(0)}_{0s\nu}|$, where $\Delta\epsilon^{(0)}_{0s\nu}$ is the distance between the level $\{0s\nu\}$ and a closest level admixed by the perturbation Hamiltonian $\hat{H}_{\rm coupl}$. With the aid of equations (2.20) and (2.27), this condition can be rewritten as

$$\frac{P_\perp^2}{2M^\perp_{s\nu}} \ll \frac{|\Delta\epsilon^{(0)}_{0s\nu}|}{\mu_{s\nu} - 1} \equiv K^{\max}_{s\nu} , \quad (2.29)$$

in terms of the "kinetic energy" of the transverse atomic motion.

2.3. *Mass Anisotropy of the Moving Hydrogen Atom*

For the hydrogen atom ($m_e \ll m_i$) one can neglect the second term in the curly brackets of equation (2.27) and put $m_i \simeq M$. Besides, at high magnetic fields one has $I^2_{0s\nu;0,s\pm1,\nu} \simeq 1$ and $I^2_{0s\nu;0,s\pm1,\nu'} \ll 1$ for $\nu' \neq \nu$. For instance, the calculations carried out with codes described by Potekhin & Pavlov (1993) show that $6 \times 10^{-3} < (1 - I^2_{000,010}) < 2 \times 10^{-2}$, $1.6 \times 10^{-4} < I^2_{000,012} < 2 \times 10^{-3}$, $3 \times 10^{-5} < I^2_{000,014} < 4 \times 10^{-4}$, etc, for $10^4 > \beta > 50$. This means that the sum over ν' is determined mainly by the term $\nu' = \nu$, in which we can replace $I^2_{00\nu,01\nu} \to 1$, so that

$$\mu_{s\nu} = \left(\frac{s+1}{a^i_{0s\nu;0,s+1,\nu} + 1} - \frac{s}{a^i_{0,s-1,\nu;0s\nu} + 1}\right)^{-1} . \quad (2.30)$$

In particular, if the atom is in one of the levels with $s = 0$, including the ground one ($s = 0$, $\nu = 0$), we obtain

$$\mu_{0\nu} = 1 + \frac{\hbar\omega_{Bi}}{\chi_{00\nu} - \chi_{01\nu}} . \quad (2.31)$$

To calculate the transverse atomic mass with these simplified equations, one needs only to know the energy spectrum of the

atom at rest, which has been investigated thoroughly in many papers. We have verified that, e.g., for the ground level, equation (2.31) gives an accuracy of at least 5% at $50 < \beta < 10^4$, compared to the more accurate equation (2.27). The numerical results discussed below were obtained from equations (2.30), (2.31), with the energies calculated in earlier papers (Rösner et al. 1984; Simola & Virtamo 1978) for $\beta \leq 1000$, and those obtained with our adiabatic code (Potekhin & Pavlov 1993) for $\beta > 1000$.

The dependence on the magnetic field of the transverse atomic mass in the $s = 0$ band is shown in Figure 1. We see that the transverse mass grows monotonically with increasing field strength for all the levels. It is much higher when the atom is excited to the hydrogen-like levels ($\nu \geq 1$) since the ionization potentials $\chi_{00\nu}$ and $\chi_{01\nu}$ are much closer to each other. However, in magnetic fields typical of neutron stars the anisotropy is not small, even for the ground level ($\mu_{00} \simeq 1.15$–1.8 for $B = 10^{12}$–10^{13} G). The field dependence of the anisotropy for the ground level can be understood from the well-known approximations (e.g., Canuto & Ventura 1977) $\chi_{0s0} \sim \mathrm{Ry} \ln^2 \beta$, and $\chi_{000} - \chi_{010} \sim \mathrm{Ry} \ln \beta$ which yield $\mu_{00} - 1 \sim 4(m_e/m_i)(\beta/\ln \beta)$. The magnetic effect on the mass is stronger for odd hydrogen-like states than for even ones. The reason is that the energies of the odd states are much closer to the corresponding field-free hydrogen levels, and the distances between the adjacent odd levels, $\chi_{00\nu} - \chi_{01\nu}$, are much less than for the even ones. Approximations for the quantum defects obtained by Hasegawa & Howard (1961) allow one to estimate $\mu_{0\nu} \sim (m_e/m_i)\nu^2\beta \ln^2 \beta$ and $\mu_{0\nu} \sim (m_e/m_i)\nu^3\beta^2 \ln^2 \beta$ for even and odd ν, respectively.

The mass anisotropy ratios for the four lowest tightly bound states ($\nu = 0$) are plotted in Figure 2. They also increase with the field and with the quantum number s. These dependences (for $\beta < 500$) have been calculated previously by Vincke & Baye (1988) with a much more complicated version of the perturbation approach.

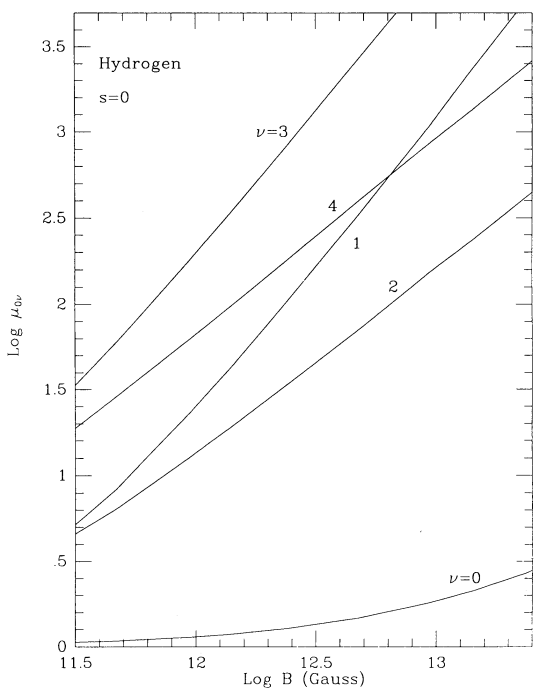

FIG. 1.—Dependence of the transverse mass of the hydrogen atom (in units of the field-free mass) on the magnetic field for different longitudinal levels ν (figures near the curves) on the $s = 0$ band.

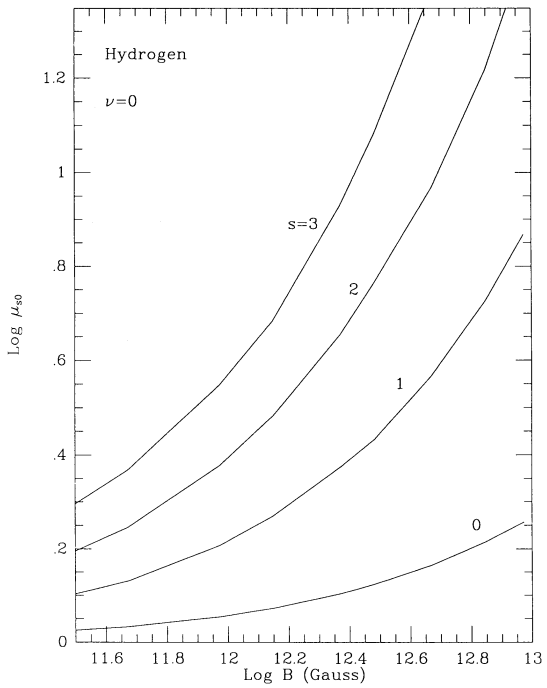

FIG. 2.—Dependence of the transverse atomic mass of the hydrogen atom on the magnetic field for tightly bound levels ($\nu = 0$) with different s (figures near the curves).

The limiting kinetic energy of the transverse atomic motion for which the perturbation treatment is still valid can be estimated from equations (2.29) (with $\Delta\epsilon^{(0)}_{0s\nu} = \chi_{0s\nu} - \chi_{0,s+1,\nu} + \hbar\omega_{Bi}$) and (2.31). In particular, for the states with $s = 0$ the limiting energy equals

$$K_{0\nu}^{\max} = \frac{(\chi_{00\nu} - \chi_{01\nu} + \hbar\omega_{Bi})(\chi_{00\nu} - \chi_{01\nu})}{\hbar\omega_{Bi}} \simeq \chi_{00\nu} - \chi_{01\nu}\,, \tag{2.32}$$

where the latter equality stands for the case $\hbar\omega_{Bi} \gg \chi_{00\nu} - \chi_{01\nu}$. As an example, for $\beta = 500$ ($B = 2.35 \times 10^{12}$ G) we obtain $K_{00}^{\max} \simeq 260$ eV, $K_{10}^{\max} \simeq 30$ eV, $K_{20}^{\max} \simeq 8$ eV, $K_{01}^{\max} \simeq 0.15$ eV, $K_{02}^{\max} \simeq 0.5$ eV, etc. We see that the limitations are rather strong, especially for the hydrogen-like levels.

Of course, the same perturbation approach can be also applied in the limit of a weak magnetic field ($\beta \ll 1$). In this case, one has the usual set of quantum numbers, $\kappa = \{n, l, m\}$. Thus, in the ground state ($n = 1$, $l = m = 0$) one has $\langle 100 | H_{\mathrm{coupl}} | 21 \pm 1 \rangle \sim e(P/Mc)Ba_0$, where a_0 is the Bohr radius, which immediately gives $M^{\perp}_{100} \sim M[1 + O(\beta^2 m_e/m_i)]$. Exact calculations give the value

$$\mu_{100} = 1 + \frac{9}{2}\frac{\hbar\omega_{Bi}}{\mathrm{Ry}}\frac{\hbar\omega_{Be}}{\mathrm{Ry}}\,. \tag{2.33}$$

We see that at $\beta \ll 1$ the anisotropy remains very low, although it grows with B faster than in the limit of very strong fields.

2.4. *The Positronium Atom*

In this case we have $m_i = m_e$, $M = 2m_e$, $\hbar\omega_{Bi} = \hbar\omega_{Be}$, and $\epsilon^{(0)}_{Nsv} = \hbar\omega_{Be}(2N + s + 1) + \epsilon^{\parallel}_{Nsv}$. The latter equality means that

all the states with $s \neq 0$ are lifted above the states with $N = 0$, $s = 0$ by an energy $\gtrsim \hbar\omega_{Be}$ and are essentially metastable (Wunner et al. 1981b, 1983). Therefore we consider only a set $|N = 0, s = 0, \nu\rangle$. Making use of the relations (Hasegawa & Howard 1961)

$$g_{Ns\nu}(z) = g_{N+s,-s,\nu}(z) , \quad \chi_{Ns\nu} = \chi_{N+s,-s,\nu} , \tag{2.34}$$

one can transform equation (2.27) for the positronium case as follows:

$$\mu_{0\nu}^{-1} = \sum_{\nu'} \frac{I^2_{00\nu,01\nu'}}{a^e_{00\nu,01\nu'} + 1} . \tag{2.35}$$

In the same approximation which we used for the hydrogen atom, $I^2_{00\nu,01\nu'} \simeq \delta_{\nu\nu'}$, equation (2.35) yields

$$\mu_{0\nu} = 1 + \frac{\hbar\omega_{Be}}{\chi_{00\nu} - \chi_{01\nu}} , \tag{2.36}$$

where $\chi_{0s\nu}$ are the negatives of the longitudinal energies for positronium. According to equation (2.28a),

$$\chi_{0s\nu}(B) = \tfrac{1}{2}\chi_{0s\nu}(4B, m_i \to \infty) . \tag{2.37}$$

The field dependence of the mass anisotropy ratio for three lowest levels of the positronium is shown in Figure 3. The mass anisotropy is seen to be much stronger in the positronium case than in the hydrogen atom since it does not contain the small factor m_e/m_i. For example, the transverse mass ratio is $\mu_{00} \simeq 740$ for $\beta = 500$. The dependence of the mass anisotropy on the magnetic field for the ground level can be approximately described as $\mu_{00} \sim 8\beta/\ln\beta$. The limiting energy of the transverse motion equals (see eq. [2.29]) $K_{0\nu}^{\max} \simeq \chi_{00\nu} - \chi_{01\nu}$, which yields, for example, $K_{00}^{\max} \simeq 30$ eV for $\beta = 500$.

3. KINEMATIC, THERMODYNAMIC, AND SPECTROSCOPIC CONSEQUENCES

3.1. *Mechanical Effects*

When the neutral atom moves in a weakly nonuniform field (where the typical inhomogeneity scales are macroscopic, and the variation of the field as seen in the comoving frame is adiabatic), the motion can be described quasi-classically, i.e., one can consider the mean coordinate, momentum, velocity, etc., as functions of time and use for these the classical equations of motion. Just as in classical mechanics, one can consider the generalized momentum $\boldsymbol{P}$ and center-of-mass position $\boldsymbol{R}$ as two canonical variables which obey Hamilton's equations,

$$\dot{\boldsymbol{R}} = \partial\mathscr{H}/\partial\boldsymbol{P} , \quad \dot{\boldsymbol{P}} = -\partial\mathscr{H}/\partial\boldsymbol{R} \tag{3.1}$$

where $\mathscr{H} = E + U$ is the Hamiltonian function, $E = -\chi + P_{\parallel}^2/2M + P_{\perp}^2/2M^{\perp} = E[\boldsymbol{P}, \boldsymbol{B}(\boldsymbol{R})]$ is the previously derived energy of the atom ($\chi > 0$ is the binding energy), and $U = U(\boldsymbol{R})$ is the potential of any external (nonmagnetic) forces. Then the first of Hamilton's equations coincides with equation (2.13), and the second one reads

$$\frac{d\boldsymbol{P}}{dt} = -\frac{\partial E}{\partial \boldsymbol{R}} + \boldsymbol{F} , \tag{3.2}$$

where $\boldsymbol{F} = -\partial U/\partial\boldsymbol{R}$ is the external force. The first term in the right-hand-side of equation (3.2) is an additional force caused by the nonuniformity of the magnetic field (we are indebted to H. Herold for a crucial clarification on this point). For an atom at rest ($\boldsymbol{P} = 0$), it is directed along the gradient of the magnetic field magnitude, $\partial B/\partial\boldsymbol{R}$. If the magnetic and external fields do not vary with time, then the Hamiltonian function is conserved, $d(E + U)/dt = 0$. If, for instance, $\boldsymbol{F} = 0$, and the magnetic field does not change its direction in the region of the motion, $\boldsymbol{B} = B(X, Y)\boldsymbol{\epsilon}_Z$, then equations (3.2) and (2.13) imply that, along the atom's trajectory,

$$V_{\parallel} = \text{const} , \quad M^{\perp}V_{\perp}^2 - 2\chi = \text{const} . \tag{3.3}$$

Since $M^{\perp}$ and χ depend on B (see § 2.2), the latter equation means that the transverse component of the mean velocity of the atom may change while the atom moves in a nonuniform magnetic field. We consider two specific examples below.

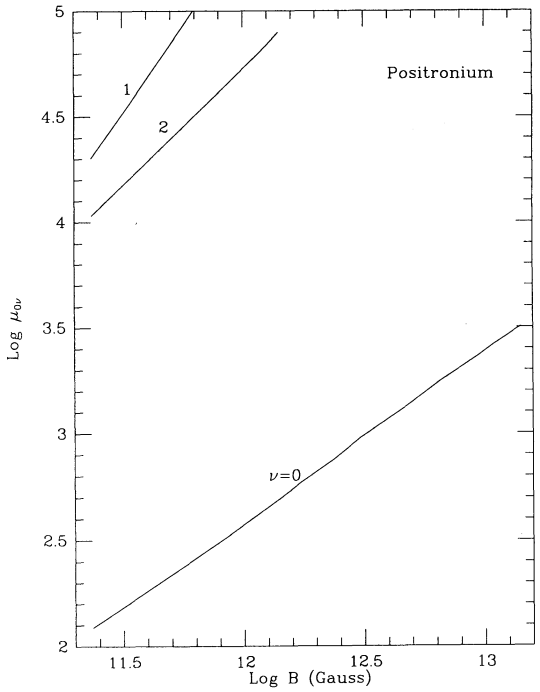

FIG. 3.—The same as in Fig. 1 for the positronium atom

3.1.1. *Refraction of an Atomic Beam*

Consider an atomic beam in the X-Z plane moving adiabatically from a uniformly magnetized region of space into another uniformly magnetized region. Let the magnetic fields $\boldsymbol{B}_1$ and $\boldsymbol{B}_2$ ($B_1 > B_2$) be parallel to the Z-axis in both regions. It follows from equation (3.3) that the beam velocities $\boldsymbol{V}_1$ and $\boldsymbol{V}_2$ in the corresponding regions are connected by the equations

$$V_{2Z} = V_{1Z} , \quad M_2^{\perp}V_{2X}^2 - 2\chi_2 = M_1^{\perp}V_{1X}^2 - 2\chi_1 , \tag{3.4}$$

$$\frac{\sin\theta_2}{\sin\theta_1} = \frac{V_1}{V_2} = \left(1 + \frac{\Delta M^{\perp}}{M_2^{\perp}}\cos^2\theta_1 - \frac{2\Delta\chi}{M_2^{\perp}V_1^2}\right)^{-1/2} \tag{3.5a}$$

$$= \left(1 - \frac{\Delta M^{\perp}}{M_1^{\perp}}\cos^2\theta_2 + \frac{2\Delta\chi}{M_1^{\perp}V_2^2}\right)^{1/2} , \tag{3.5b}$$

where θ_1 and θ_2 are the angles with respect to the X-axis, i.e., the normal to the boundary (following the convention used in optics of refractive media, not to be confused with the usual magnetic notation where θ is respect to the magnetic field direction), $\Delta\chi = \chi_1 - \chi_2 > 0$ is the difference in binding energies, and $\Delta M^{\perp} = M_1^{\perp} - M_2^{\perp} > 0$.

Let us look first at a beam going from a region of stronger field B_1 toward one of lower field B_2. According to the second

of equations (3.4), the beam cannot penetrate into the lower field region at any incidence angle θ_1 if $M_1^{\perp}V_1^2 < 2\Delta\chi$. This means that the kinetic energy of the beam is too low to overcome the potential barrier formed by the difference of the binding energies even at normal incidence $\theta_1 = 0$. The beam is reflected, changing the sign of the tranverse velocity V_{1X}. However, if $M_1^{\perp}V_1^2 > 2\Delta\chi$, there exists an angle of total internal reflection θ_r,

$$\cos^2\theta_r = \frac{2\Delta\chi}{M_1^{\perp}V_1^2} \tag{3.6}$$

such that the beam is reflected from the lower magnetic field region for incidence angles $\theta_1 > \theta_r$ (see the trajectory $a \rightarrow a$ in Fig. 4), but is able to penetrate through the boundary if $\theta_1 < \theta_r$. In the latter case the beam is deflected from its original direction toward the boundary, $\theta_1 < \theta_2 < \pi/2$ for any θ_1 if $\Delta M^{\perp}V_1^2 < 2\Delta\chi$ (e.g., the trajectory $b_1 \rightarrow b_2$). If, however, $\Delta M^{\perp}V_1^2 > 2\Delta\chi$, there exists a critical angle θ_c,

$$\cos^2\theta_c = \frac{2\Delta\chi}{\Delta M^{\perp}V_1^2} = \frac{2\Delta\chi}{\Delta M^{\perp}V_2^2}, \tag{3.7}$$

such that the beam is deflected toward the boundary for $\theta_1 > \theta_c$ (the trajectory $b_1 \rightarrow b_2$), and toward the X-axis ($0 < \theta_2 < \theta_1$) for $\theta_1 < \theta_c$ (the trajectory $c_1 \rightarrow c_2$).

Consider now an atomic beam going from a region of weaker field B_2 toward a region of stronger field, B_1. In this case the beam is able to penetrate through the boundary for all angles of incidence θ_2. It follows from equation (3.5b) that if $\Delta M^{\perp}V_2^2 < 2\Delta\chi$, then $\theta_1 < \theta_2$ for any θ_2. If the inverse inequality is fulfilled, we obtain $\theta_2 < \theta_1 < \theta_c$ for $\theta_2 < \theta_c$ (the trajectory $c_2 \rightarrow c_1$), and $\theta_c < \theta_1 < \min(\theta_2, \theta_r)$ for $\theta_2 > \theta_c$ (the trajectory $b_2 \rightarrow b_1$).

Let us consider now the case when the beam moves in the X-Y plane perpendicular to the magnetic field. Since $\partial E/\partial Y = 0$, we have $dP_Y/dt = 0$, and

$$M_2^{\perp}V_{2Y} = M_1^{\perp}V_{1Y}, \quad M_2^{\perp}V_2^2 = M_1^{\perp}V_1^2 - 2\Delta\chi, \tag{3.8}$$

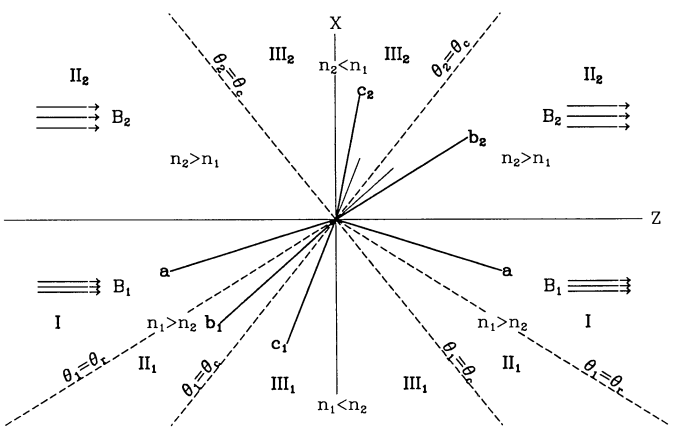

FIG. 4.—Refraction of the atomic beams a, b, c traveling in two uniformly magnetized regions in the X-Z plane. Magnetic fields $\boldsymbol{B}_1$ and $\boldsymbol{B}_2$ are parallel to the Z-axis ($B_1 > B_2$). The beam velocities, transverse masses, and binding energies are assumed to be such that $\Delta M^{\perp}V_1^2 > 2\Delta\chi$, $\Delta M^{\perp}V_2^2 > 2\Delta\chi$. The angles of total internal reflection θ_r and critical angle θ_c are given by eq. (3.6) and (3.7). Note that transitions of the beam are allowed only between the regions $I \leftrightarrow I$, $II_1 \leftrightarrow II_2$, and $III_1 \leftrightarrow III_2$; n_1 and n_2 are the velocity-dependent "refraction indices" in different regions.

$$\frac{\sin\theta_2}{\sin\theta_1} = \frac{V_{2Y}}{V_{1Y}}\frac{V_1}{V_2} = \left(\frac{M_1^{\perp}}{M_2^{\perp}}\right)^{1/2}\left(1 - \frac{2\Delta\chi}{M_1^{\perp}V_1^2}\right)^{-1/2} = \left(\frac{M_1^{\perp}}{M_2^{\perp}}\right)^{1/2}\left(1 + \frac{2\Delta\chi}{M_2^{\perp}V_2^2}\right)^{1/2}. \tag{3.9}$$

The beam can enter the region of lower field B_2 only if $M_1^{\perp}V_1^2 > 2\Delta\chi$. If this condition is fulfilled, the beam is deflected toward the boundary, $\theta_2 > \theta_1$. On the other hand, the beam can enter the region of higher field B_1 at any V_2, deflecting away from the boundary $\theta_1 < \theta_2$.

These neutral atomic beam direction changes show some partial resemblance to the phenomenon of light refraction. The main difference is that the "refractive index" is not only dependent on medium properties (e.g., the field strength) but also on the velocity of the beam. For instance, in the example shown in Figure 4, the beam moving toward the boundary in the regions I and II_1 ($\theta_1 > \theta_c$) "meets" the lower field region as having a lower refractive index, $n_2 < n_1$, whereas $n_2 > n_1$ for $\theta_1 < \theta_c$ (i.e., for the incident beam in the region III_1). The picture is naturally reversed for a beam entering the larger field region: $n_1 < n_2$ for $\theta_2 > \theta_c$ (region II_2), and $n_1 > n_2$ for $\theta_2 < \theta_c$ (region III_2).

3.1.2. *Trajectory Bending in a Nonuniform Magnetic Field*

Take the magnetic field to be of the form $\boldsymbol{B} = B(X)\boldsymbol{\epsilon}_Z$, $dB/dX > 0$, and let the atom be at the coordinate origin at $t = 0$. Then the conservation of P_Z, P_Y, and E yields the following equations of motion

$$Z = V_{0Z}t, \quad Y = V_{0Y}\int_0^t dt\,\frac{M_0^{\perp}}{M^{\perp}[X(t)]}, \tag{3.10}$$

$$\int_0^X dX\left(\frac{M^{\perp}}{M_0^{\perp}}\right)^{1/2}\left(1 + \frac{M^{\perp} - M_0^{\perp}}{M^{\perp}}\frac{V_{0Y}^2}{V_{0X}^2} + \frac{2\Delta\chi}{M_0^{\perp}V_{0X}^2}\right)^{-1/2} = V_{0X}t, \tag{3.11}$$

where $M_0^{\perp} = M^{\perp}(X = 0)$, $\Delta\chi = \chi(X) - \chi(0)$. Given the dependence of B on X (and thereby $M^{\perp}[X]$ and $\Delta\chi[X]$), one can find $\boldsymbol{R}(t)$ from these equations, as well as the equation for the trajectory.

If $V_{0Y} = V_{0Z} = 0$, the motion is one-dimensional along the X-axis. If, for instance, $V_{0X} < 0$, the atom starts to move in the negative X direction, slowing down due to a force caused by the decreasing binding energy ($\Delta\chi < 0$ for $X < 0$). It changes the direction of the motion at a point where $2|\Delta\chi| = M_0^{\perp}V_{0X}^2$ and accelerates toward positive X. Since the transverse mass grows with increasing B faster than the binding energy (see § 2.3), the acceleration eventually decreases and turns into deceleration, while the atom keeps going along the gradient of B.

If $V_{0Y} = 0$ or $V_{0Z} = 0$, the motion is two-dimensional in the X-Z or X-Y plane, respectively. In the X-Z plane, the trajectory equation is

$$Z = \frac{V_{0Z}}{V_{0X}}\int_0^X dX\left(\frac{M^{\perp}}{M_0^{\perp}}\right)^{1/2}\left(1 + \frac{2\Delta\chi}{M_0^{\perp}V_{0X}^2}\right)^{-1/2}. \tag{3.12}$$

The shape of the trajectory near the origin depends essentially on the sign and magnitude of V_{0X}. For sufficiently large t, the motion along X slows down due to the growth of the transverse mass so that the trajectory bends toward the direction of the magnetic field lines, $d^2X/dZ^2 < 0$, independently of the

initial conditions. When the atom moves in the X-Y plane, it accelerates due to the gradient of the binding energy in the X direction and decelerates due to the growth of the transverse mass in both the X and Y directions. As a result, the trajectory bends toward the gradient of the magnetic field, $d^2X/dY^2 > 0$.

If both V_{0Y} and V_{0Z} differ from zero, the trajectory is three-dimensional. It bends simultaneously toward both the magnetic field lines and the direction of the magnetic field gradient.

The simple examples considered above illustrate some of the general features of the atomic motion in a nonuniform magnetic field: the atoms tend to bend their trajectories, on the one hand, toward the direction of the field gradient, due to a force caused by the dependence of the binding energy on B, and on the other hand, toward the magnetic field lines, due to the anisotropy of the mass of the atoms. If the directions of the gradient and of the field itself are close to each other, as in the important case of atoms near the pole of a magnetic dipole, then both effects conspire together to make the atoms bend their trajectories in the same direction, i.e., toward the polar region. It should be emphasized that such trajectory bending in a nonuniform magnetic field is inevitable also when the atomic motion is driven by external nonmagnetic forces.

3.1.3. *Magnetic Forces in Magnetized Atmospheres*

Since the energy of the neutral atom depends on the magnetic field, an additional "magnetic" force is exerted on the atom in any nonuniform magnetic field (see eq. [3.2]). This means that an additional term, proportional to the gradient of the energy averaged over a Maxwell-Boltzmann distribution (see § 3.2) should be added into the equation of hydrostatic equilibrium for a magnetized stellar atmosphere. Since the averaged energy $\langle E \rangle$ does not depend on the direction of the magnetic field, the equilibrium equation reads

$$\frac{\partial \mathscr{P}}{\partial \boldsymbol{R}} = \rho \boldsymbol{g} - N_a \frac{\partial \langle E \rangle}{\partial B} \frac{\partial B}{\partial \boldsymbol{R}}, \tag{3.13}$$

where N_a is the number density of atoms. Since $\langle E \rangle = \langle \chi \rangle$ in the perturbation approach, the force is proportional to the gradient of the mean binding energy. If the typical length scale for the magnetic nonuniformity is R_M, the ratio of the magnetic force to the gravitational force can be estimated as

$$\frac{f_m}{f_g} \sim \frac{R_*^2\,\mathrm{Ry}}{GMM_* R_M} \frac{B}{\mathrm{Ry}} \frac{\partial \langle \chi \rangle}{\partial B} \simeq 10^{-7} \times \left(\frac{R_*}{10\ \mathrm{km}}\right)\left(\frac{M_\odot}{M_*}\right)\left(\frac{R_*}{R_M}\right) \frac{B}{\mathrm{Ry}} \frac{\partial \langle \chi \rangle}{\partial B}. \tag{3.14}$$

If the atoms are mostly on the ground level, then $(B/\mathrm{Ry})(\partial\langle\chi\rangle/\partial B) \sim 2 \ln \beta$ at $\beta \gg 1$, and $\sim 2\beta^2$ at $\beta \ll 1$.

Although the magnetic force is much smaller than the gravitational force (if $R_M \sim R_*$), its absolute value may be rather high, $f_m \sim 3 \times 10^7 (N_a/10^{23}\ \mathrm{cm}^{-3})(10\ \mathrm{km}/R_*)$ dyn cm^{-3} for $\beta \sim 1000$. The magnitude of this force could be even higher if for some reason $R_M \ll R_*$, e.g., if the field is nondipole, or has a small-scale structure induced, e.g., by migration (Ruderman 1991), thermomagnetic effects (Blandford, Applegate, & Hernquist 1983) or initial conditions. What is more important, it has a component orthogonal to the gravitational force. This means that pressure, density, and temperature in the atmosphere are constant not at the spherical surfaces of constant gravitational potential but at the nonspherical surfaces of constant total (gravitational + "magnetic") potential. For instance, in the dipole magnetic field case the tangential component of the force is directed from the equator toward nearest pole, being zero at both the equator and poles. This results in an increase of the density and pressure at the poles as compared with those at the equator at the same radius. It is well known (see, e.g., Schwarzschild 1958) that the heat balance in such nonspherical atmospheres can be maintained only if there is some flow of matter in the meridional planes, i.e., meridional circulation.

3.2. *Thermodynamic Effects*

According to equation (2.23), a Maxwell-Boltzmann distribution of a hydrogen gas can be written as

$$f_\kappa(\boldsymbol{P}) = Z^{-1} \exp\left\{-\frac{1}{kT}\left[\frac{P_z^2}{2M} + \frac{P_\perp^2}{2M_\kappa^\perp} + \epsilon_\kappa^{(0)}\right]\right\}, \tag{3.15}$$

where

$$Z = \int_{-\infty}^{+\infty} dP_\parallel \exp\left(-\frac{P_\parallel^2}{2MkT}\right) \times \int_0^\infty 2\pi P_\perp\, dP_\perp \sum_\kappa \exp\left[-\frac{P_\perp^2}{2M_\kappa^\perp kT} - \frac{\epsilon_\kappa^{(0)}}{kT}\right] = (2\pi MkT)^{3/2} \sum_\kappa \frac{M_\kappa^\perp}{M} \exp\left[-\frac{\epsilon_\kappa^{(0)}}{kT}\right], \tag{3.16}$$

is the partition function. Since we used the perturbation approach, which is not valid at high temperatures (see eq. [2.32]), this expression for Z can be directly applied when the temperature is sufficiently low that only the ground level is populated. Equation (3.15) implies that the distributions of the atomic momenta and velocities in a given "internal" state κ are anisotropic. The average values of the longitudinal components remain the same as in the absence of a magnetic field, while the transverse components become

$$\langle P_\perp \rangle = \sqrt{2M_\kappa^\perp kT} > \langle P_\parallel \rangle; \quad \langle V_\perp \rangle = \sqrt{2kT/M_\kappa^\perp} < \langle V_\parallel \rangle. \tag{3.17}$$

Equation (3.16) means that the atomic partition function in the magnetic field increases its value over that which would be calculated for the atom at rest. Since the fraction of nonionized atoms is proportional to the partition function, the ionization degree decreases with respect to what is expected without allowance for the mass anisotropy.

3.3. *Radiative Effects*

3.3.1. *Changes of the Oscillator Strengths and Selection Rules*

A more direct effect on the opacities is due to the fact that the change of the wave functions due to the motion of the atoms should change both the oscillator strengths of radiative processes and the applicable selection rules. The selection rules change due to an admixture of states with $s' = s \pm 1$, which means, in particular, that the motion allows additional transitions which are forbidden for the fixed atom (as considered until now). Consider, for instance, the absorption of the left-polarized quanta propagating along the magnetic field (this polarization is responsible for the electron cyclotron absorption by free electrons) from the states with $N_i = 0$, $s_i = 0$. The quanta may be absorbed only if the atom goes to a state with $s_f = -1$. Such states exist only for $N_f \geq 1$; that is, without motion, the absorption is allowed only for very high frequencies, $\omega \geq \omega_{Be} - \omega_{Bi} + (\epsilon_{1-1\nu_f}^\parallel - \epsilon_{00\nu_f}^\parallel)/\hbar \simeq \omega_{Be}$. This means that at low temperatures, when only the ground state is

populated and atoms are not ionized, the gas is transparent to the extraordinary normal wave, which causes some (artificial) troubles, e.g., in modeling neutron star atmosphere spectra at UV temperatures, such as are relevant for cooling pulsars being now observed by *ROSAT*. If the motion is taken into account, the states with $s = 1$ are admixed to $s_i = 0$, and transitions to $N_f = 0$, $s_f = 0$ become allowed. Applying the standard expression for the wave function in the first order of the perturbation theory to general formulae for the photoionization cross section in the adiabatic approximation (Potekhin & Pavlov 1993), we obtain the cross section for the left circular polarization (superscript " − ") given by

$$\sigma^{-}_{00\nu_i\to 00\nu_f} = \pi\alpha\,\frac{\hbar^2 P_\perp^2}{2M^2}\,\frac{|I_{00\nu_f,01\nu_i}|^2}{(\hbar\omega_{Bi}+\chi_{00\nu_i}-\chi_{01\nu_i})^2}\,\frac{\hbar\omega}{\sqrt{\epsilon_f\,\mathrm{Ry}}}\,\frac{L}{a_B}\,, \tag{3.18}$$

where $\alpha = e^2/\hbar c$, $I_{00\nu_f,01\nu_i}$ is the overlapping integral of the longitudinal wave functions of the initial (bound) and final (continuum) states, ϵ_f is the longitudinal energy of the final state, a_B is the Bohr radius, and L is the normalization length along the z-direction of the final state. Comparing this with, e.g., the cross section for the right circular polarization from the state $\{01\nu_i\}$ of a fixed atom (Potekhin & Pavlov 1993), we get (for equal values of ϵ_f)

$$\frac{\sigma^{-}_{00\nu_i\to 00\nu_f}}{\sigma^{+}_{01\nu_i\to 00\nu_f}} = \frac{P_\perp^2}{4M}\,\frac{\hbar\omega_{Bi}}{(\hbar\omega_{Bi}+\chi_{00\nu_i}-\chi_{01\nu_i})^2} \sim \frac{K_{0\nu_i}}{K^{\max}_{0\nu_i}}\,, \tag{3.19}$$

where $K_{0\nu_i} = P_\perp^2/2M^\perp_{0\nu_i}$ and $K^{\max}_{0\nu_i}$ is given by equation (2.32). Note that, when averaged over a Maxwellian distribution, the cross section (3.18) is proportional to the temperature of the gas.

3.3.2. *One-Photon Positronium Annihilation*

Another interesting consequence of the change of the selection rules occurs in the case of positronium, for which one-photon annihilation now becomes possible. This process is forbidden by the conservation of energy and momentum if the positronium mass is isotropic (Wunner et al. 1981b). However, with allowance for the mass anisotropy, the conservation law is

$$2m_e c^2 + \frac{P_z^2}{2M} + \frac{P_\perp^2}{2M^\perp_{0\nu}} - \chi_{00\nu} = \hbar\omega\,, \tag{3.20a}$$

$$\boldsymbol{P} = \hbar\boldsymbol{q}\,, \tag{3.20b}$$

where $M = 2m_e$, $q = \omega/c$, gives for the energy of the annihilation photon

$$\hbar\omega = \frac{2m_e c^2}{\cos^2\theta + (M/M^\perp_{0\nu})\sin^2\theta} \times\left[1-\sqrt{1-\left(2-\frac{\chi_{00\nu}}{m_e c^2}\right)\left(\cos^2\theta+\frac{M}{M^\perp_{0\nu}}\sin^2\theta\right)}\right], \tag{3.21}$$

where θ is the angle between $\boldsymbol{q}$ and the magnetic field. It follows from this that the annihilation is allowed only if

$$\cos^2\theta \le \frac{m_e c^2}{2m_e c^2-\chi_{00\nu}}\,\frac{M^\perp_{0\nu}}{M^\perp_{0\nu}-M} - \frac{M}{M^\perp_{0\nu}-M}\,, \tag{3.22}$$

which, in turn, is possible when

$$\frac{M^\perp_{0\nu}}{M} > 2 - \frac{\chi_{00\nu}}{m_e c^2}\,. \tag{3.23}$$

The latter inequality is fulfilled even in not very strong magnetic fields, $\beta \gtrsim 1$, e.g., in old millisecond pulsars. In the typical fields of the more standard neutron stars, we have $M^\perp_{0\nu} \gg M$ (see § 2.4), which leads to an obvious simplification of the equations (3.21) and (3.22). When $\cos\theta$ varies from zero to the maximum value, the energy of the created photon increases from $2m_e c^2 - \chi_{00\nu}$ to $2(2m_e c^2 - \chi_{00\nu})$.

3.3.3. *Spectral Line Width and Photoionization Edge Changes*

The atomic lines and photoionization edges suffer additional shifts and broadening due to the magnetic mass anisotropy Consider, for instance, the bound-bound absorption process $|1\rangle + \hbar\omega \to |2\rangle$. With allowance for the momentum conservation, $\boldsymbol{P}_2 = \boldsymbol{P}_1 + \hbar\boldsymbol{q}$, the energy of the absorbed photon obeys the following equation:

$$\begin{aligned}\hbar\omega = E_2 - E_1 &= \epsilon_2^{(0)} - \epsilon_1^{(0)} + \frac{(P_{1z}+\hbar q_z)^2}{2M} - \frac{P_{1z}^2}{2M} \\ &+ \frac{(\boldsymbol{P}_\perp+\hbar\boldsymbol{q}_\perp)^2}{2M_2^\perp} - \frac{P_{1\perp}^2}{2M_1} \simeq \epsilon_2^{(0)} - \epsilon_1^{(0)} \\ &+ \frac{P_{1z}\hbar\omega\cos\theta}{Mc} + \frac{P_{1\perp}\hbar\omega\sin\theta\cos\varphi}{M_2^\perp c} \\ &+ \frac{P_{1\perp}^2}{2}\left(\frac{1}{M_2^\perp}-\frac{1}{M_1^\perp}\right),\end{aligned} \tag{3.24}$$

where θ is the angle between the wave vector $\boldsymbol{q}$ and the magnetic field, and φ is the angle between the $\boldsymbol{Bq}$ and $\boldsymbol{BP}_1$ planes. The third and fourth terms in equation (3.24) are the modified Doppler shift while the last term is the "magnetic" shift induced by the mass anisotropy (or, in other words, by the different dependences of the binding energies on the generalized momentum). Being averaged over a thermal distribution of generalized momenta $\boldsymbol{P}_1$ (cf. eq. [3.15]),

$$f(\boldsymbol{P}_1) = \frac{1}{(2\pi MkT)^{3/2}}\,\frac{M}{M_1^\perp}\exp\left(-\frac{P_{1z}^2}{2MkT}-\frac{P_{1\perp}^2}{2M_1^\perp kT}\right), \tag{3.25}$$

the shifts becomes the modified Doppler width

$$\begin{aligned}\Gamma_D &= \omega\sqrt{\frac{2kT}{Mc^2}}\sqrt{\cos^2\theta+\frac{MM_1^\perp}{(M_2^\perp)^2}\sin^2\theta} \\ &= \sqrt{(\Gamma_D^\parallel)^2+(\Gamma_D^\perp)^2}\,,\end{aligned} \tag{3.26}$$

and the magnetic width is

$$\Gamma_M = \frac{kT}{\hbar}\left(1-\frac{M_1^\perp}{M_2^\perp}\right). \tag{3.27}$$

The modification of the Doppler width due to mass anisotropy has been mentioned by Wunner et al. (1983) who, however, assumed $M_1^\perp = M_2^\perp$. As a numerical example, for the states $|1\rangle = |s=0,\ \nu=0\rangle$ and $|2\rangle = |s=1,\ \nu=0\rangle$ at $\beta = 500$ ($B = 2.35\times10^{12}$ G) we have $\epsilon_2^{(0)} - \epsilon_1^{(0)} = 55$ eV, $M_1 = 1.27M$, $M_2 = 2.37M$, $\hbar\Gamma_M = 0.47kT$, $\hbar\Gamma_D = 0.025(kT/100\ \text{eV})^{1/2}(\cos^2\theta + 0.23\sin^2\theta)^{1/2}$ eV. For $kT = 20$ eV this gives $\hbar\Gamma_M = 9.4$ eV, $\hbar\Gamma_D = 0.011(\cos^2\theta + 0.23\sin^2\theta)^{1/2}$ eV, and $\Gamma_M/\Gamma_D \gtrsim 800$.

The (normalized) line profile can be obtained by averaging $\delta(\hbar\omega - E_2 + E_1)$ over the momentum distribution,

$$F(\omega) = \pi^{-3/2}\int_{-\infty}^{\infty} du\,e^{-u^2}\int_0^\infty dv\,ve^{-v^2} \times\int_0^{2\pi} d\varphi\,\delta(\Delta\omega - u\Gamma_D^\parallel - v\Gamma_D^\perp\cos\varphi + v^2\Gamma_M), \tag{3.28}$$

where

$$\Delta\omega = \omega - [\epsilon_2^{(0)} - \epsilon_1^{(0)}]/\hbar\,, \quad u = P_{1z}(2MkT)^{-1/2}\,,$$
$$v = P_{1\perp}(2M_1^{\perp}kT)^{-1/2}\,.$$

For $\theta = 0$ integration yields

$$F(\omega) = \frac{1}{2\Gamma_M}\exp\left(\frac{\Delta\omega}{\Gamma_M} + \frac{\Gamma_D^2}{4\Gamma_M^2}\right)\operatorname{erfc}\left(\frac{\Delta\omega}{\Gamma_D} + \frac{\Gamma_D}{2\Gamma_M}\right). \quad (3.29)$$

This has the asymptotic shape

$$F(\omega) = \begin{cases} \pi^{-1/2}\left[\Gamma_D + \left(\frac{2\Gamma_M}{\Gamma_D}\right)\Delta\omega\right]^{-1}\exp\left[-\left(\frac{\Delta\omega}{\Gamma_D}\right)^2\right], \\ \qquad \text{if } \Delta\omega > 0\,, \quad \frac{\Delta\omega}{\Gamma_D} + \frac{\Gamma_D}{2\Gamma_M} \gg 1\,; \\ \Gamma_M^{-1}\exp\left[-\left(\frac{|\Delta\omega|}{\Gamma_M}\right) + \left(\frac{\Gamma_D^2}{4\Gamma_M^2}\right)\right], \\ \qquad \text{if } \Delta\omega < 0\,, \quad \left|\frac{\Delta\omega}{\Gamma_D} + \frac{\Gamma_D}{2\Gamma_M}\right| \gg 1\,. \end{cases} \quad (3.30)$$

Thus, while the typical drop-off half-width blueward of $\Delta\omega = 0$ is characterized by Γ_D, the redward half-width is given by the much larger Γ_M, which therefore dominates the total width and is the most important broadening mechanism. At other angles θ the profile has a similar asymmetric shape, its magnetic width being independent of θ and the Doppler width decreasing gradually with increasing θ.

Analogous considerations are applicable to the case of bound-free (photoionization) edges. Since atoms in highly excited states have very large transverse mass (in other words, the lower boundary of the continuum is independent of $\boldsymbol{P}$), we can put $M_2^{\perp} \to \infty$ in the above expressions for the widths,

$$\Gamma_D = \omega\sqrt{\frac{2kT}{Mc^2}}\cos\theta\,, \quad \Gamma_M = \frac{kT}{\hbar}\,. \quad (3.31)$$

This means that the edges are broadened mainly redward, with a typical width Γ_M.

4. DISCUSSION AND ASTROPHYSICAL APPLICATIONS

The effects of a finite velocity on the structure and properties of neutral atoms and ions in a strong magnetic field discussed here are of potentially significant importance for the atmospheric structure, energy balance, and spectral properties of neutron stars, in particular isolated cooling neutron stars, radio pulsars, and accreting X-ray pulsars. The perturbation method used to describe these effects is valid only within a range of (relatively low) temperatures (see eq. [2.32] and estimates below). However, it has the advantage of being significantly simpler than a nonperturbative approach, and it is amenable to a quantitative solution of the problem in analytic form, allowing the investigation of a number of interesting departures from the previously known lore of atomic physics in pulsar atmospheres.

The main microphysical effect that the allowance for atomic motion induces in the (strongly magnetized) atom is an effective anisotropy of the mass between the directions parallel and transverse to the magnetic field. This is caused by the fact that the perfect cylindrical symmetry enjoyed by the stationary magnetized atom is broken by the presence of the finite electric field induced by the motion of the center of mass. The anisotropy grows with the magnetic field, being much stronger for excited atomic levels.

One intriguing consequence of these effects is the fact that a beam of neutral atoms will be refracted upon entering a region of high magnetic field, with "refraction indices" depending on the velocity of the incident atoms, while for atoms trying to move out of a region of high field there exists an angle of incidence beyond which total internal reflection occurs so that they remain in the high field region (§ 3.1.1). This is due to the competing effects of an increased binding energy and an increased transverse mass in the high field region. Neutral atoms moving in an inhomogeneous magnetic field will have their trajectory bent (§ 3.1.2). For motion in a plane containing the magnetic field direction the trajectory bends closer to the field, while for motion in a plane perpendicular to the field there is a tendency to bend in the direction of the gradient of the field. This phenomenon is of interest for the problem of the gravitational accretion of neutral matter onto dead radio pulsars, or onto accreting X-ray pulsars along directions where the ionizing radiation flux is not significant or is self-absorbed. Previously, it was thought that neutral matter, if accreted, would ignore the magnetic field and fall in radially. The present result, however, indicates that neutral matter will have a tendency to gradually align its motion along the field lines. As a result, both ionized *and* neutral matter would tend to accumulate onto the magnetic polar caps, contrary to previous assumptions. Another consequence (§ 3.1.3) is that neutral atoms in the atmosphere of a neutron star or a magnetic white dwarf will be subjected to an anisotropic magnetic volume force directed toward the poles or toward the regions of higher field, which may cause meridional circulation in the atmospheres of these stars.

Another consequence, which could influence the analysis of many types of neutron stars (even those with fields as low as those in millisecond pulsars and possibly X-ray bursters, e.g., $B \gtrsim 10^9$ G), is the fact that the ionization balance in the atmosphere could be significantly different from that previously thought to exist (§ 3.2). The physical reason for this is that the level-dependent anisotropic mass enters the effective momentum that describes the distribution function, and through that the partition function which is used to calculate Saha's equation for the ionization balance. The conventional *Ansatz* has previously been to take most ions, particularly the low-mass ones, to be completely ionized in the atmospheres of X-ray radiating neutron stars. The ionization state of the atmosphere is a major element in the modeling of the soft X-ray emission of cooling pulsar atmospheres (Romani 1987; Miller 1992; Shibanov et al. 1992, 1993; Ventura et al. 1992, 1993). A reliable knowledge of the state of ionization is required for any quantitative work on the interpretation of the observations of such objects. Perhaps of even more far reaching consequences, the usual assumption of completely ionization of H and He in all types of X-ray emitting neutron stars may need to be reevaluated. If a fraction as small as 10^{-5} of the H and/or He were neutral, the effects could be significant at X-ray energies, since the frequency dropoff of the opacities in a magnetic field above the ionization edges is more gradual than in the free-field case (Gnedin, Pavlov, & Tsygan 1974; Potekhin & Pavlov 1993).

Several distinctive soft X-ray spectroscopic features are expected as a result of the mass anisotropy. Aside from the possible signature of H and He bound-free continua, qualitatively new effects appear because of changes in the selection rules and in the oscillator strengths of both bound-free and

bound-bound transitions (§ 3.3.1). If the atoms were stationary, the left-hand polarized photons (which are the most abundant ones) can be absorbed from the low-lying $N_i = 0$, $s_i = 0$ states only by states with $N_f \geq 1$, which represents a very large jump in energy for reasonable pulsar fields, so this polarization would be essentially free to escape unhindered. The breaking of the symmetry by the finite motion, however, makes the $\Delta N = 0$ transitions allowed in the moving atom, with the consequence that photons with this (most important) polarization are subject to a finite opacity. This causes in the diffusion regime a significant buildup of the photon density above the main ionization threshold, changing substantially previous estimates of the spectral fluxes and the polarization of the thermal-like radiation from neutron stars.

At gamma-ray energies, an interesting prediction is that of the existence of a new channel for positronium annihilation introduced by the finite velocity. In this case, the one-photon annihilation of positronium (which is forbidden for the stationary positronium) becomes kinematically allowed, and involving only one photon vertex its cross section is expected to be significantly larger in sufficiently strong magnetic fields than that for two- or three-photon annihilation. The energy of the photon is also twice that of the two-photon annihilation and could give rise to some of the lines observed near 1 MeV (previously ascribed to single-photon annihilation of free e^+e^- pairs, e.g., Teegarden & Cline (1981). This mechanism could also be of importance in the consideration of photon-positronium state mixing in pulsars, or "photon-trapping" (e.g., Usov & Shabad 1985; Herold, Ruder, & Wunner 1985), which has been invoked to explain the presence of high-energy gamma rays in pulsars at angles relative to the magnetic field larger than the kinematic limit for one-photon annihilation of unbound e^+e^- pairs.

The energies of the photoionization edges and bound-bound lines of neutral atoms, which are dependent on the magnetic field strength, are also affected by the finite atomic velocity. The mass anisotropy modifies the Doppler widths of the edges and lines, and the dependence of the anisotropy on the level number causes a new type of very strong, asymmetric broadening, with predominance of the long-wavelength wing (§ 3.3.2). Thus, both the edge and line shifts and widths are dependent on a combination of the magnetic field strength and the temperature. An independent determination of the temperature (e.g., through continuum spectrum atmosphere modeling) would then allow a determination of the magnetic field strength from the edge or line positions and widths. Current observations at soft X-ray energies (e.g., with *ROSAT* or *EUVE*) may be able to detect such features in cooling pulsars, in particular from relatively high-flux objects such as PSR 0656+14 (Finley, Ögelman, & Kiziloglu 1992) or Geminga (Halpern & Holt 1992).

We are grateful to J. Ventura, D. Yakovlev, A. Potekhin, and V. Bezchastnov for useful discussion, and to the referee, H. Herold, for a careful reading and valuable comments. Our special thanks are due to Alexander Potekhin for providing the codes to calculate the energy levels and overlapping integrals in strongly magnetized hydrogen. This research has been partially supported through NASA NAGW-1522.

REFERENCES

Avron, J. E., Herbst, I. W., & Simon, B. 1978, Ann. Phys., 114, 431
Blandford, R. D., Applegate, J., & Hernquist, L. 1983, MNRAS, 204, 1025
Canuto, V., & Ventura, J. 1977, Fund. Cosmic Phys., 2, 203
Finley, J. P., Ögelman, H., & Kiziloglu, Ü. 1992, ApJ, 394, L21
Gnedin, Yu. N., Pavlov, G. G., & Tsygan, A. I. 1974, Soviet Phys.—JETP, 39, 301
Gor'kov, L. P., & Dzyaloshinskii, I. E. 1968, Soviet Phys.—JETP, 26, 449
Hasegawa, H., & Howard, R. E. 1961, J. Phys. Chem. Solids, 21, 179
Halpern, J., & Holt, S. S. 1992, Nature, 357, 222
Herold, H., Ruder, H., & Wunner, G. 1981, J. Phys. B, 14, 751
———. 1985, Phys. Rev. Lett., 54, 1452
Mészáros, P. 1992, High-Energy Radiation from Magnetized Neutron Stars (Chicago: Univ. of Chicago Press)
Miller, M. C. 1992, MNRAS, 255, 109
Nagase, 1989, PASJ, 41, 1
Potekhin, A. Yu., & Pavlov, G. G. 1993, ApJ, 407, 330
Romani, R. 1987, ApJ, 313, 718
Rösner, W., Wunner, G., Herold, H., & Ruder, H. 1984, J. Phys. B, 17, 29
Ruderman, M. 1974, in IAU Symp. 53, Physics of Dense Matter, ed. C. Hansen (Dordrecht: Reidel), 117
Ruderman, M. 1991, ApJ, 366, 261
Schwarzschild, M. 1958, Structure and Evolution of Stars (Princeton: Princeton Univ. Press)
Shibanov, Yu. A., Zavlin, V. E., Pavlov, G. G., & Ventura, J. 1992, A&A, 266, 313
Shibanov, Yu. A., Zavlin, V. E., Pavlov, G. G., Ventura, J., & Potekhin, A. Yu. 1993 in Isolated Pulsars, ed. K. A. Van Riper, R. I. Epstein, & C. Ho (Cambridge: Cambridge Univ. Press), 174
Simola, J., & Virtamo, J. 1978, J. Phys. B, 11, 3309
Teegarden, B., & Cline, T. 1981, Ap&SS, 75, 181
Usov, V. V., & Shabad, A. E. 1985, Soviet Phys.—JETP Lett., 42, 19
Ventura, J., Herold, H., Ruder, H., & Geyer, F. 1992, A&A, 261, 235
Ventura, J., Shibanov, Yu. A., Zavlin, V. E., & Pavlov, G. G. 1993, in Isolated Pulsars, ed. K. A. Van Riper, R. I. Epstein, & C. Ho (Cambridge: Cambridge Univ. Press), 168
Vincke, M., & Baye, D. 1988, J. Phys. B, 21, 2407
Wunner, G., Herold, H., & Ruder, H. 1983, J. Phys. B, 16, 2937
Wunner, G., Ruder, H., & Herold, H. 1981a, ApJ, 247, 374
———. 1981b, J. Phys. B, 14, 765